HIGH ENERGY CRYSTALLINE LASER MATERIALS

R. C. Ohlmann, et al

Westinghouse Research Laboratories
Pittsburgh, Pennsylvania

December 1967

HIGH ENERGY CRYSTALLINE LASER MATERIALS

Final Technical Summary Report
16 October 1967 to 3 March 1967

1 December 1967

Contract Nonr-4658(00)
ARPA Order No. 306
Code 4730

R. C. Ohlmann, Principal Investigator
R. Mazelsky
J. Murphy

HIGH ENERGY CRYSTALLINE LASER MATERIALS

Final Technical Summary Report
16 October 1967 to 3 March 1967

1 December 1967

Contract Nonr-4658(00)
ARPA Order No. 306
Code 4730

R.C. Ohlmann, Principal Investigator
R. Mazelsky
J. Murphy

TABLE OF CONTENTS

ABSTRACT

A potential high energy laser material, $GdAlO_3$ doped with chromium, is discussed in terms of its growth problems and spectroscopic characteristics. Crystals have been pulled from the melt, but difficulties in maintaining stoichiometry during growth have not been completely solved. The fluorescence of Cr^{3+} has an 18 msec decay time and a broad R-line. The width and structure of the R-lines are theoretically described as due to the ferromagnetic exchange interactions with neighboring Gd^{3+} ions.

OBJECTIVES

To investigate crystals which show potential as high power laser materials, the study to include both spectroscopic measurements and the development of crystal growth techniques. The ultimate objective is to discover a laser crystal that is capable of a greater total output energy in a Q-spoiled laser mode than presently available materials.

Summary

The study has concentrated on oxide crystals doped with chromium in which the chromium R-line fluorescence has a long decay time and/or a broad line width so that laser gain will be sufficiently low to prevent saturation due to amplified spontaneous emission. Crystalline materials that meet these requirements are lanthanum aluminate ($LaAlO_3$), gadolinium aluminate ($GdAlO_3$), and magnesium aluminum spinel ($MgAl_2O_4$), all doped with chromium.

The studies on these materials showed that $LaAlO_3$:Cr has sharp emission lines having a 76 ms lifetime (77°K), $GdAlO_3$:Cr has broad lines ($\sim$ 50A) having an 18 ms lifetime, and $MgAl_2O_4$:Cr has broad lines ($\sim$ 80A) having a 12 ms lifetime. Crystal growth of $LaAlO_3$ did not result in good quality crystals due to a phase transition at 425°C which causes domains to form, although work by another contractor showed that it may be possible to improve the quality of these crystals after growth by applying uniaxial pressure. No phase transition occurs in $GdAlO_3$ but the results of Czochralski growth have not been completely satisfactory, possibly because of the purity of the starting materials. Work on $MgAl_2O_4$ growth has been pursued by another contractor.

Spectroscopic studies revealed that concentrations of chromium as high as 0.5 atomic percent can be incorporated into $LaAlO_3$ and $GdAlO_3$ without excessive absorption. This is significant since it means high energy storage per unit volume is possible in a Q-spoiled laser of these materials.

A basic study of chromium-gadolinium interactions in $GdAlO_3$ was conducted. Since Gd^{3+} has a half-filled f shell, there is a ferromagnetic exchange interaction between each Cr^{3+} ion and its eight Gd^{3+} nearest cation neighbors. Our theoretical work indicates that the line width and shape of the R line fluorescence is due to this interaction. Crossrelaxation across the emission line is much faster than the decay time. It has not yet been determined whether the emmision can be considered homogeneously broadened in the time range of a few nanoseconds, as required in a Q-spoiled laser.

In addition to the study of chromium fluorescence, the transfer of energy from chromium to neodymium in $LaAlO_3$, $GdAlO_3$, and $Y_3Al_5O_{12}$ (yttrium aluminum garnet) was investigated. Rapid and efficient transfer occurs in $LaAlO_3$ and $GdAlO_3$, while the transfer rate is somewhat slower in $Y_3Al_5O_{12}$. The efficiency of neodymium-doped lasers can be appreciably increased by sensitizing with chromium.

The major results during this contract period are adequately described in two papers which are being submitted for publications. These papers are included as Appendix A and B. Earlier results on Cr^{3+} in other hosts and on the transfer of energy from Cr^{3+} to Nd^{3+} are described in the previous Annual Report of the same title dated 15 November 1965, and in the Semiannual Report dated 15 May 1965.

Future Research

Crystal growth efforts on $GdAlO_3$ and $MgAl_2O_4$ should be continued until sufficient quality is attained to first demonstrate laser action and then to determine the energy storage capabilities. When good crystals of $GdAlO_3$ are available laser action using neodymium doping should also be tested. The fast decay time of neodymium

(∿ 140 μsec) will not allow a long pump pulse to be used. However, the low gain of neodymium in this material and the high efficiency obtained by sensitizing with chromium should allow a high efficiency, high repetition rate Q-spoiled laser output.

In addition to the above materials we have successfully used an efficient high gain material, $Ca_5(PO_4)_3F$:Nd in Q-spoiled operation. Large crystals of good quality have been grown. Related apatite-structure hosts with lower gain show promise for efficient high repetition rate lasers and crystal growth, spectroscopic studies and laser tests should be conducted on them.

BLANK PAGE

APPENDIX A

THE SPECTRUM OF Cr^{3+} IN $GdAlO_3$*

R. C. Ohlmann† and J. Murphy

I. INTRODUCTION

Exchange interactions between rare earth ions and transition metal ions in insulating solids have not yet been studied very extensively. In compounds containing a high concentration of transition metal ions, the exchange interaction between these ions has the dominant effect on the magnetic susceptibility so that it becomes difficult to determine the weaker rare earth-transition metal exchange interaction. Spectroscopic studies,[1] both in the visible and in the infrared spectral regions, have revealed some direct information on these weaker interactions, particularly between rare earth ions and Fe^{3+}. In these experiments[2-5] the perturbations of the rare earth ion energy levels (as observed by optical absorption) due to the exchange interactions with the magnetically ordered transition metal ions were examined. In some cases the perturbation can be described[6] by the molecular field theory, although the details require a spin wave treatment including anisotropy and higher order coupling. In the case of highly anisotropic exchange interactions it has been necessary to consider an exchange potential rather than an exchange constant to describe the spectra. The studies do not extend to the paramagnetic region ($T > T_N$) since the strong exchange between the transition metal ions results in a high Neél temperature, and the spectral lines of the rare earth ions become too broad to observe structure in the spectrum.

In order to study rare earth-transition metal ion exchange interactions at low temperatures and without the complication of strong interactions between the transition metal ions, materials have been chosen containing low concentrations of the transition metal ions. Since trivalent chromium has some sharp spectral lines in many crystals, it has been used as a probe in the rare earth

aluminates. The magnetic properties of some of the rare earth aluminates have been recently determined,[8] and spectral studies revealing the exchange interactions between rare earth ions have been recently reported.[9,10] These compounds tend to order magnetically below 4°K. Therefore, to a first approximation, the exchange interactions between the rare earth ions are considered small compared to the chromium-rare earth exchange, an assumption justified by the experimental results.

In this paper the characteristics of the optical spectra of Cr^{3+} in $GdAlO_3$ are reported and analyzed. In a previous publication[11] we briefly described the fluorescence spectra of Cr^{3+} in $GdAlO_3$ but did not include much data on the absorption spectra. The gross features of the absorption spectrum are typical of that found for Cr^{3+} surrounded by six oxygen ions in almost octahedral symmetry. However the R-lines due to $^2E - {}^4A_2$ transitions are broad and consist of two bands in absorption and four bands in fluorescence. Our interpretation is based on the exchange interaction between each Cr^{3+} ion and the surrounding cluster of eight nearest Gd^{3+} ions. Blazey and Burns[12] recently reported similar fluorescence spectra from Cr^{3+} in $GdAlO_3$, but their analysis contains significant conceptual differences from ours, and these lead to somewhat different results. These differences are discussed in Sec. VI.

$GdAlO_3$ has a distorted perovskite-type structure[13] (D_{2h}^{16} - Pbnm) which is isostructural with $GdFeO_3$. The simple cubic perovskite unit cell may be visualized as a cube having eight Gd^{3+} ions at the corners and an Al^{3+} ion at the body center, and having six O^{2-} ions at the center of the faces. The true orthorhombic structure of $GdAlO_3$ has four formula units per unit cell, although all Al^{3+} ions are at crystallographically equivalent sites which only have inversion symmetry. The distortion of the unit cell from a simple cubic structure is small since a pseudocell may be constructed with sides 3.731, 3.731, 3.734 (A) and corner angle of 90.6°. The principal indices of refraction[14] are 1.991, 2.004, and 2.151. Small amounts of Cr^{3+} will preferentially substitute for Al^{3+} in $GdAlO_3$.

In our theoretical treatment we assume that the optical spectra can be adequately described by the approximation of a simple cubic perovskite structure with Cr^{3+} in octahedral symmetry.

II. EXPERIMENTAL TECHNIQUES

Preparation of Samples

The initial studies were conducted on ceramic samples prepared by the solid state reaction of Al_2O_3, Gd_2O_3 and Cr_2O_3, in proportion to make $GdAl_{1-x}Cr_xO_3$, with x having values from 0.0001 to 0.005. The starting materials were ground, fired at 1450°C in air, reground and refired. There was always some small quantity of ruby in the resultant powder, as evidenced by the distinctive fluorescence of the R-lines from Cr^{3+} in Al_2O_3. However, x-ray powder patterns detected only $GdAlO_3$. Reflection spectra showed the tail of a broad band absorption in the blue and ultraviolet probably due to color centers. This absorption could be reduced but not eliminated by heating in a hydrogen atmosphere.

Single crystal samples containing about 0.1 at. % Cr were prepared by the Czochralski technique. They were pulled at 2030°C from the melt contained in iridium crucibles. Although Laue x-ray photographs from each end of the boules appeared to show a single orientation, sufficient strain or twinning was present so as to make polarization studies impossible. A crystal purchased from Union Carbide (Linde Division), although of good optical quality, also could not be used with polarizers. The fluorescence spectra from both ceramic and single crystals had identical appearance except that no ruby R-lines were detected from the single crystals and, of course, the lines due to near pairs of Cr^{3+} ions were stronger at higher chromium concentrations.

Apparatus

Absorption spectra of the single crystals were measured on a Cary Model 14 spectrometer modified to increase the dynamic damping and thus the time constant. This allowed the measurement of absorption of the crystals while they were immersed in boiling helium to

insure thermal contact. Noise was also reduced by using liquid helium below its λ-point. The Cary spectrometer also had a tungsten iodide cycle lamp and a special phototube with an S-20 response.

Fluorescence measurements were made using a Jarrell-Ash 1 m Ebert grating monochromater (600 ℓ/mm) blazed at 7500A. Crystals were excited by a 1-kW AH 6 high pressure mercury lamp, and the fluorescence detected at the exit slit by, a cooled RCA 7102 photomultiplier or by an EMI 9558 photomultiplier. The photon sensitivity of the system vs wavelength was determined using a standard lamp. Fluorescence measurements were also made on a 0.5 m Jarrell-Ash grating spectrometer with automatic analog correction for the spectral sensitivity.

Excitation spectra were obtained by exciting the fluorescence with monochromatic wavelength obtained using a 900 W Hanovia xenon short-arc lamp, and a 0.5 m grating monochrometer. In order to correct for the variation of the exciting light with wavelength, part of the radiation was reflected off a clear quartz disc just before it illuminated the sample. The reflected radiation was incident on a constant-quantum-efficiency and highly absorbing detector, either a cell containing Rhodamine B in water (for $\lambda < 6000$A) whose fluorescence through the cell was then detected, or a silicon diode (for $5000 < \lambda < 10{,}000$A). The fluorescence signal was divided by this reference signal so that the excitation spectra obtained are proportional to the fluorescence per incident photon rate.

All low temperature fluorescence measurements were made with the sample immersed in the cryogenic fluid. Tests of linearity of the fluorescence with exciting intensity showed that contact was maintained with the thermal bath.

III. EXCITATION AND ABSORPTION SPECTRA

Experimental Results

Although the fluorescence of Cr^{3+} in $GdAlO_3$ around 7280A is the principal concern of this paper, the absorption spectra and the excitation spectra of the fluorescence will first be presented and analyzed in order to show that Cr^{3+} is nearly octahedrally surrounded by oxygen ions, and to compare the phenomenological crystal field parameters with those from other materials.

Figure 1 illustrates the excitation spectrum of the fluorescence at 7280A from $GdAlO_3$ containing 0.5 at. % Cr obtained at 77°K. The structure has been labeled with the most probable energy states in octahedral symmetry by comparison with the spectra of Cr^{3+} in other crystals.[15] This sample was highly absorbing at the peak of the $^4T_1$ and $^4T_2$ bands which causes their peak intensities to be almost equal. The lines due to absorption into $^2T_1$ are present and have unusually strong intensity. The spectrum also shows evidence of the excitation of the chromium fluorescence by absorption by Gd^{3+} ions which then transfer energy to the Cr^{3+} ions. Absorption lines due to transitions into the upper states of Gd^{3+} have been observed but will not be discussed in this paper.

The absorption spectrum measured on a single crystal sample at 2.2°K is shown in Figure 2. The absorption bands due to Cr^{3+} are superimposed on the long tail of a strong ultraviolet absorption band. Absorption into this band, whose absorption coefficient is 20 cm^{-1} and still rising at 39,000 cm^{-1}, is not effective in exciting Cr^{3+} fluorescence. A similar strong ultraviolet absorption is observed in $LaAlO_3$ and has been attributed to a type of vacancy.[16]

The two strong bands correspond to the $^4A_2 \rightarrow {}^4T_2$ and $^4A_2 \rightarrow {}^4T_1$ transitions. The $^4T_2$ band shows considerable vibronic structure on low energy wing which extends almost to the peak of the band. There is an uncertainty of at least $\pm$ 100 cm^{-1} in locating the peaks of both the $^4T_2$ and $^4T_1$ bands due to their width and the structure on the $^4T_2$ band. The peak energies[17] are listed in Table I.

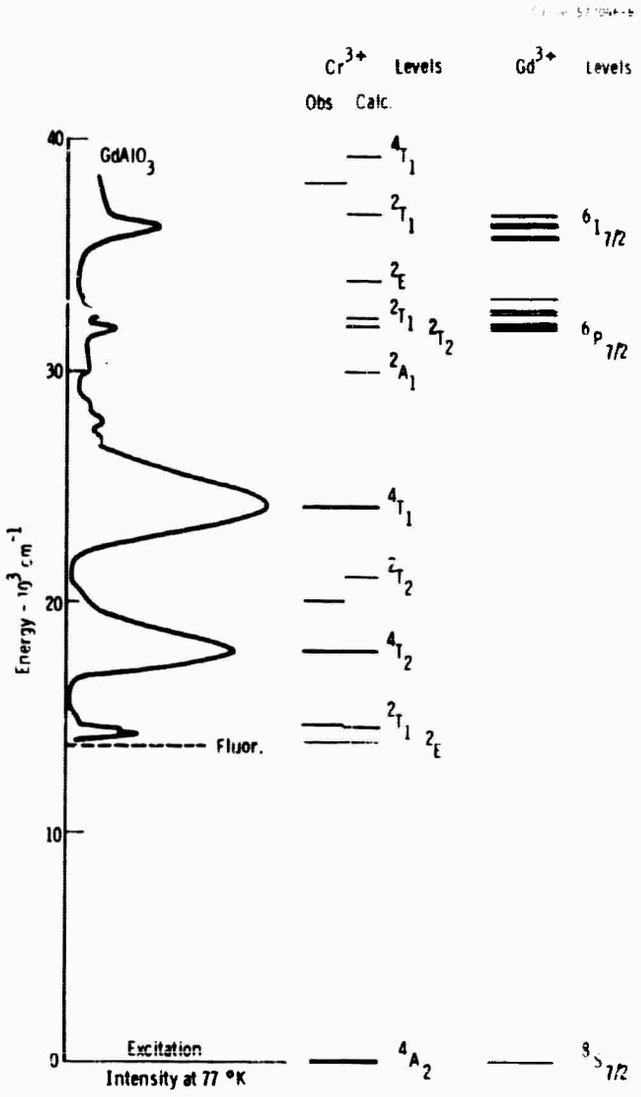

Figure 1

Excitation Spectrum of Cr^{3+} Fluorescence in $GdAlO_3$ at 77°K

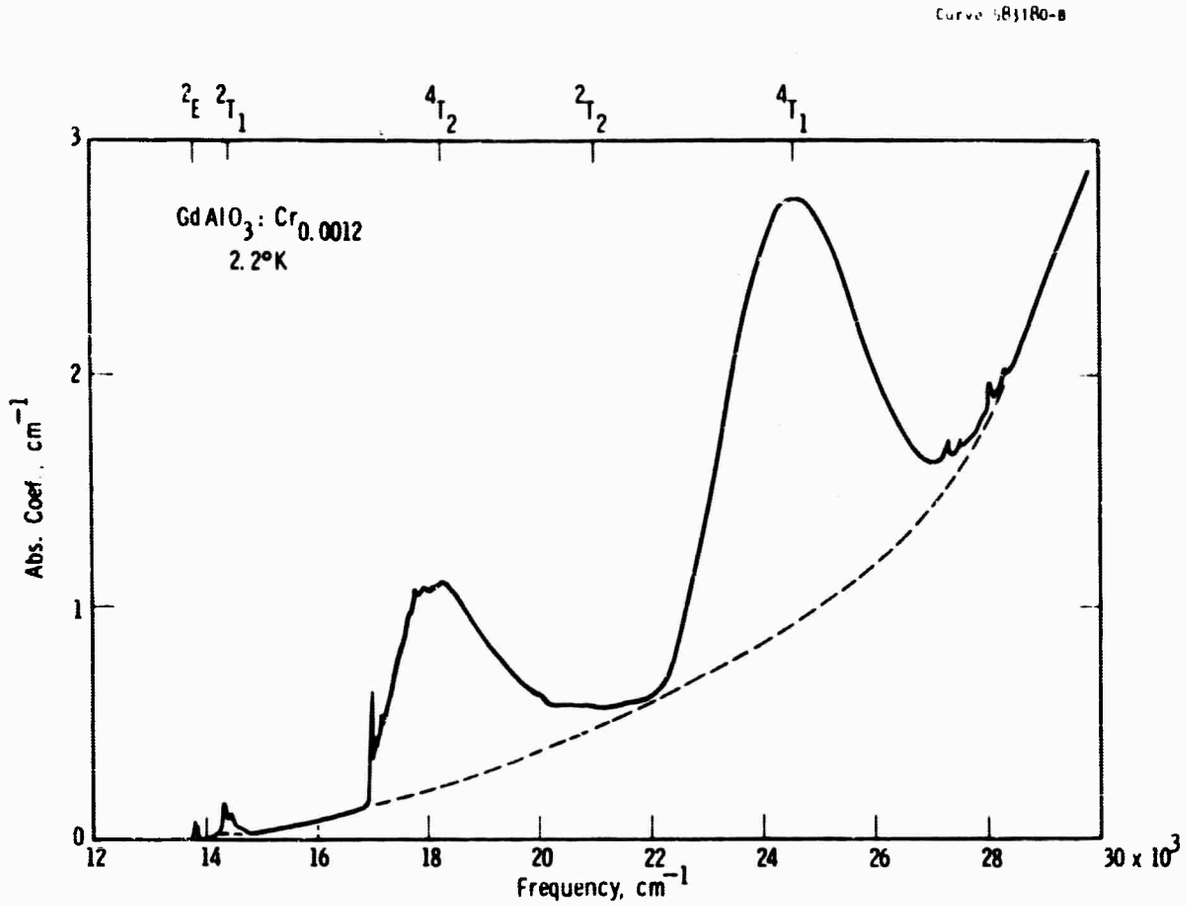

Figure 2

Absorption Spectrum of $GdAlO_3$:Cr.0012 at 2.2°K

Weak lines appear at 27248, 27285, 27502, 28011, and 28280 cm^{-1} in absorption and are also evident in the excitation spectrum. Although they lie near the energies of the higher doublet states of Cr^{3+}, transitions to these doublet states are expected to be broad and weak, and therefore unobservable. The weak lines are likely to be due to an unidentified rare-earth impurity (other than Eu^{3+} which has been investigated in $GdAlO_3$). Very weak lines also appear at 19970 and 20034 cm^{-1}. These have been tentatively identified as due to $^4A_2 \rightarrow {}^2T_2$ transitions, although they also may arise from a rare-earth impurity. Their intensities are an order-of-magnitude weaker than the lines due to transitions to the lowest doublet states, ^2E and $^2T_1$.

The absorption spectra due to $^4A_2 \rightarrow {}^2T_1$ and $^4A_2 \rightarrow {}^2E$ transitions are shown on an expanded scale in Figure 3 and 4 respectively. These figures show that both the peak and integrated absorption coefficients of these lines increase considerably as temperature is decreased, although no change of the quartet bands was observed. This effect may be due to the antiferromagnetic ordering of Gd^{3+} ions and will be discussed further in Section V.

The observed absorption lines, their integrated cross section and their oscillator strengths are listed in Table I. For the oscillator strength, f, we used the relation[18]

$$f = \frac{9n}{(n^2+2)^2} \left(\frac{mc^2}{\pi e^2} \right) \int \sigma d\bar{\nu}, \qquad (1)$$

where n is the index of refraction ($n \approx 2$).

The lifetime of the emission at several wavelengths across the band (roughly 10 Å separations) was measured and decay time was found to be independent of wavelength. It was observed that the decay time increases with temperature from helium temperatures to 77°K and decreases between 77°K and room temperature. This is consistent with the measured temperature dependence of the integrated area under the ^2E absorption curve. The lifetimes and integrated areas are related by the formula[18]

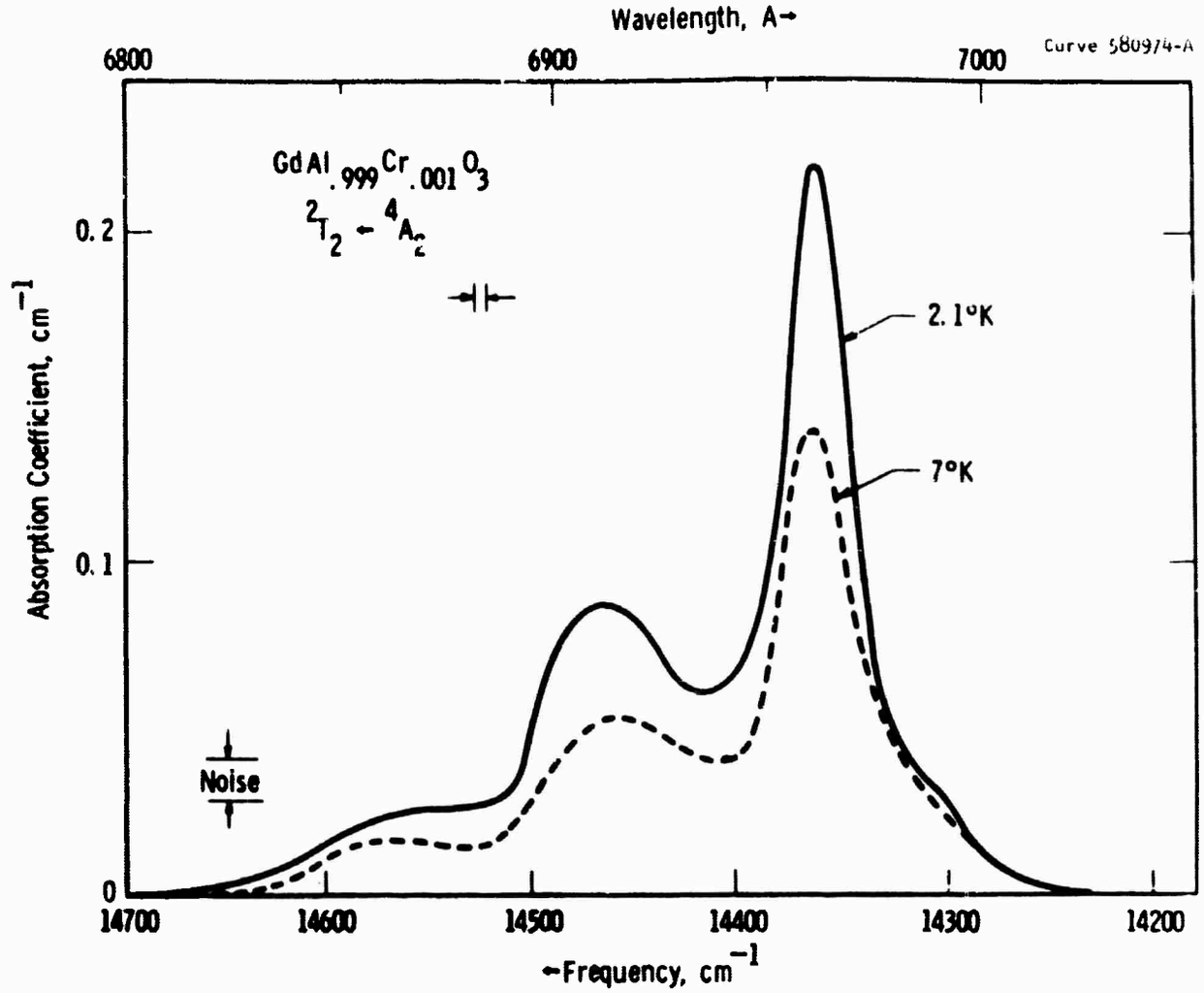

Figure 3

Details of the $^2T_2 \leftarrow {}^4A_2$ Absorption of $GdAlO_3$:Cr.001 at 2.1° and 7°K

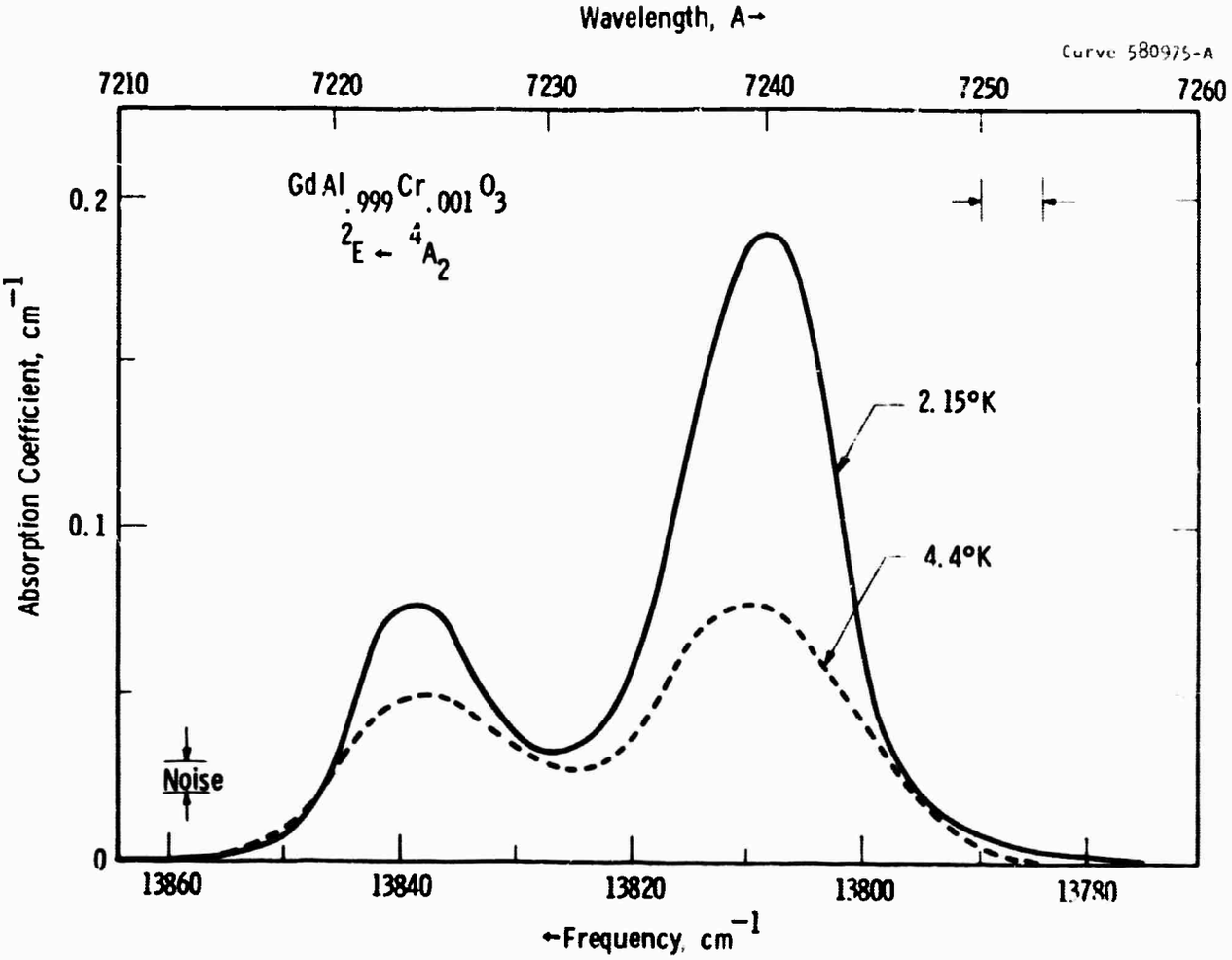

Figure 4

Details of the $^2E \leftarrow {}^4A_2$ Absorption of $GdAlO_3$:Cr.001 at 2.15° and 4.4°K

$$\frac{1}{\tau} = 8\pi\bar{\nu}^{-2}n^2c\,\frac{g_\mu}{g_L}\int \sigma d\bar{\nu} \qquad (2)$$

where $\bar{\nu}$ is the average emission frequency, n is the index of refraction of the crystal g_μ and g_L are the upper and lower state degeneracies. (Both Cr^{3+} states have a degeneracy of 4 in this case.) The results are listed in Table II along with the measured lifetimes.

Crystal Field Parameters

It is well-known that the simple crystal field model is a very incomplete description of transition metal ions in solids. However, as McClure has pointed out,[19] the values of Δ, B, and C obtained when the matrices of Tanabe and Sugano[20] are solved using the experimentally determined energy levels are very useful phenomenological parameters. Since the ^2E level of Cr^{3+} in $GdAlO_3$ is about 5% lower in energy than it is in most other compounds,[15] it is useful to determine the crystal field parameters and compare them with those found for Cr^{3+} in other oxides.

From the matrices for d^3 in a cubic field the value of Δ is the energy of the $^4T_2$ state (all energies are referred to the $^4A_2$ ground state), and B is determined by solving a 2x2 matrix involving Δ and the $^4T_1$ energy. Simply considering the propagation of errors shows that a 1% cm^{-1} uncertainty in experimentally determining the peak of $^4T_2$ and $^4T_1$ bands leads to about 9% uncertainty in B. The value of C was found by diagonalizing the ^2E matrix on a computer using the previously calculated value of B, and fitting to the mean ^2E energy as observed in the absorption spectra. The parameters with their uncertainties[21] are $\Delta = 18{,}200 \pm 100$, $B = 605 \pm 25$, and $C = 3085 \pm 75$ cm^{-1} which gives $\gamma (= C/B) = 5.1 \pm .3$.

It is to be noted from Table I that the observed positions of the levels other than those used to derive the values of the parameters are in fair agreement with the calculated values. Better agreement is not to be expected because of the approximations made.

Ignoring the errors introduced by the neglect of the spin-orbit interaction, it is well known[22] that a better fit to the free ion data can be obtained by including configurational mixing arising from the electron-electron interactions. Because of the depression of higher configurations when an ion is placed in a solid, it is reasonable to expect that such mixing effects would be even more important in crystalline spectra.

Another important effect that occurs in crystals is the mixing of metal ion wave function with those of the ligands. With this modification of the wave functions, the electron interactions are reduced because the electrons are spread out over a larger volume of space than they are without the mixing. The relative contributions of configurational mixing and convalency to the variation of the spectroscopic parameters from crystal to crystal is uncertain, however there is sufficient evidence[23] from EPR and optical experiments that admixture of ligand orbitals with metal orbitals, i.e., covalency, is necessary to account for the observed properties of metal-ligand complexes. The fluorescence spectrum of Cr^{3+} to be presented in the next section shows a coupling between the Cr^{3+} ion and the nearest neighbors gadolinium ions. There are various mechanisms by which these ions could be coupled together. If an exchange interaction is responsible, as is probably the case, the chromium electrons spend some time around the gadolinium centers. This implies a further expansion of the chromium charge cloud resulting in a reduction of the B and C parameters. The correlation between the reduction of B and C with the existence of exchange coupling of the Cr-Gd system is made only to point out the consistency of the two observations. In Table II we show by way of comparison, the B and C parameters for Cr^{3+} in various hosts as well as the Slater parameter F_2 and F_4.

IV. FLUORESCENCE SPECTRA

The fluorescence spectra of $GdAlO_3$ containing 0.2 at. % Cr is shown in Figure 5. The band near 7350A arises from pairs of Cr^{3+} ions since its intensity increases quadratically with chromium concentration. The principal feature of the spectrum is the fluorescence of the R lines due to transitions nominally labeled $^2E \rightarrow {}^4A_2$. The fluorescence of Cr^{3+} in a related perovkite, $LaAlO_3$, consists[16,24] of two sharp lines split by 5.4 cm^{-1}. Therefore, it is not reasonable to assume that the overall width (> 100 cm^{-1}) and structure of the R lines in $GdAlO_3$ are due to crystal field and spin-orbit coupling effects.

The change in fluorescence spectrum when going from 4.2° to 77°K is roughly what is expected if both ^2E bands, about 31 cm^{-1} apart as seen in absorption, participated in the fluorescence. The more diffuse nature of the spectrum at 77°K is due to both the overlap of two bands and the 20 cm^{-1} width of each ^2E band.

The fluorescence spectrum also changes shape between 4.4°K and 2.15°K as shown in Figure 6. This change was also noted by Blazey and Burns[12] who plotted the positions of the three major peaks vs temperature. Extrapolation of their data toward lower temperatures indicate that the lines do not converge at 0°K but rather near -2°K. The changes in the spectra in this region occur because of the ordering of the Gd^{3+} ions and the direction of the changes are qualitively understood as discussed in Section VI.

There is an overlap of the wings of the absorption and fluorescence spectra even at 2.2°K as illustrated in Figure 7. This overlap appears to be 20-25 cm^{-1} or about 15 kT. The overall Stokes shift between absorption and fluorescence we do not believe is due to the absorption and emission of lattice phonons but rather arises naturally in our theory of the effect of Cr^{3+} -Gd^{3+} exchange interactions.

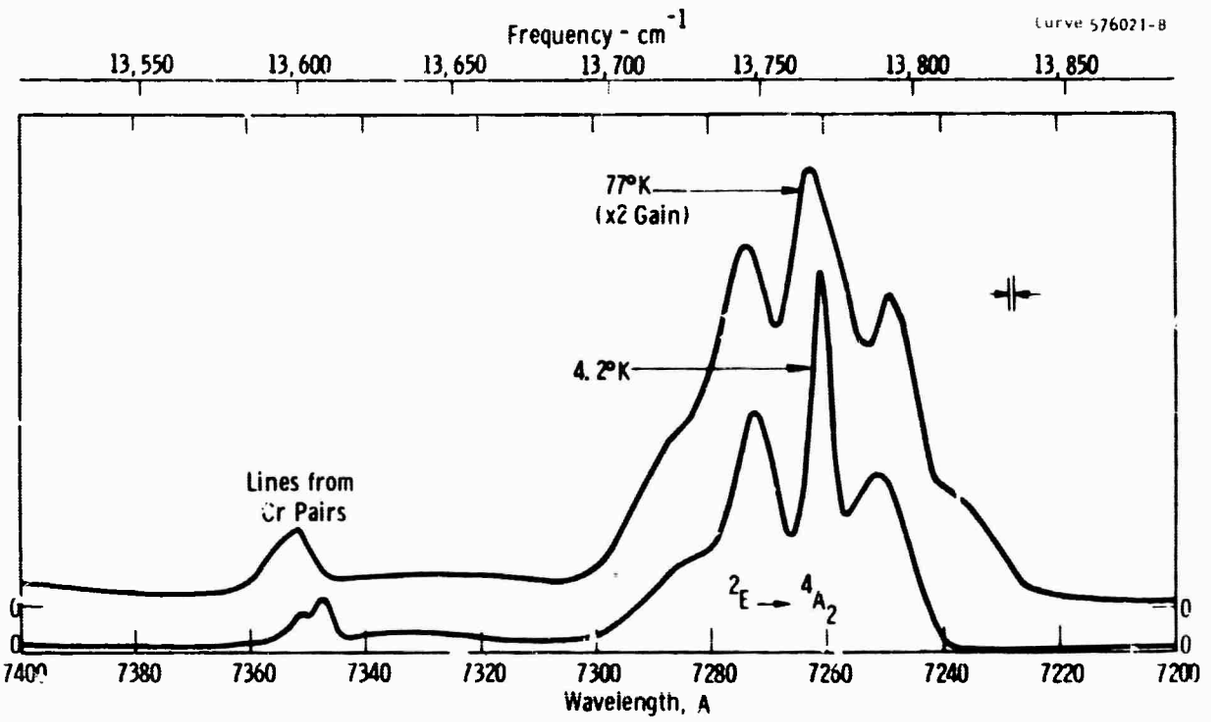

Figure 5

Fluorescence Spectra of $GdAlO_3$:Cr.002 at 4.2° and 77°K

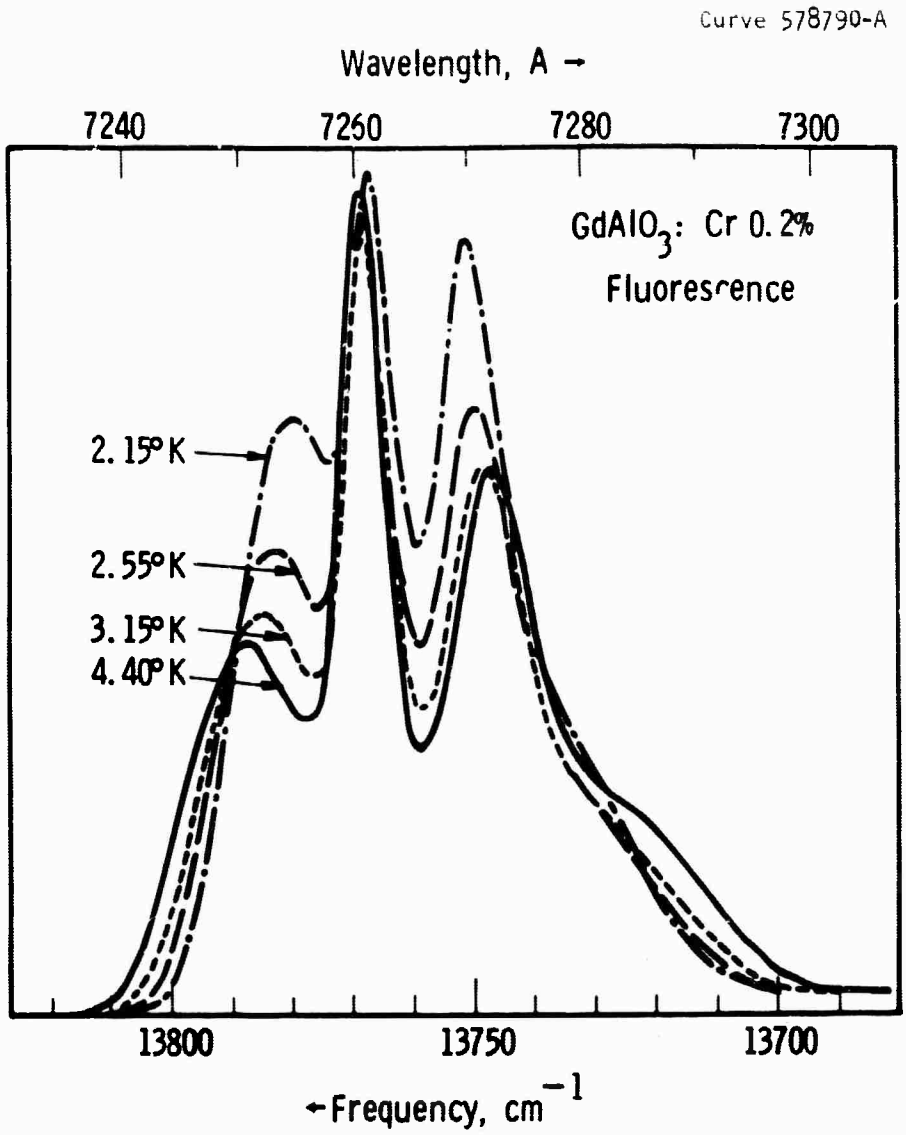

Figure 6

The Effect of Temperature on the Fluorescence of $GdAlO_3$:Cr.002 between 2.15° and 4.4°K

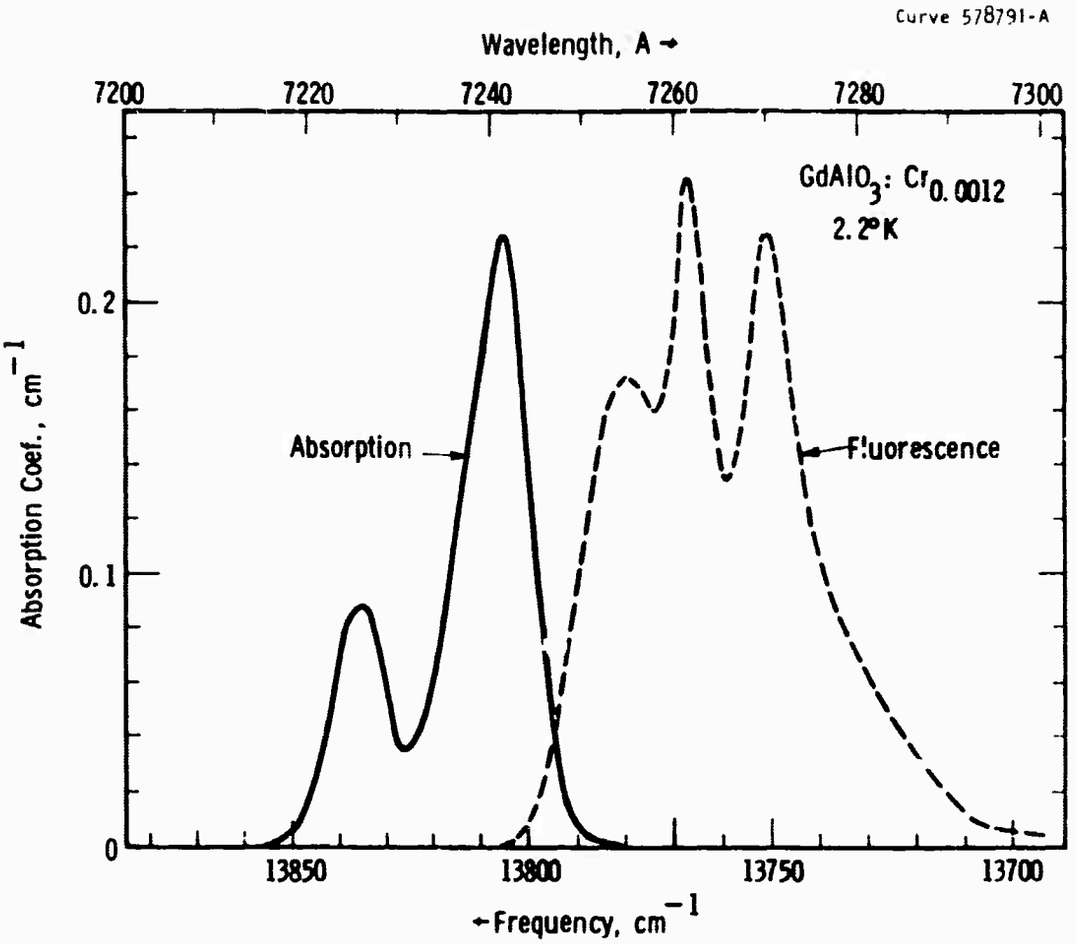

Figure 7

The Absorption and Fluorescence of $GdAlO_3$:Cr.0012
2.2°K Showing Overlap

V. EXCHANGE INTERACTIONS

In this section, we will show that the observed fluorescence spectrum of Cr^{3+} in $GdAlO_3$ bears a strong resemblance to the energy distribution of states for a Cr^{3+} ion in its ground state coupled to a system of eight Gd^{3+} ions. The coupling is assumed to be an isotropic exchange interaction of the form.

$$H' = - \Sigma J_i \vec{S}_c \cdot \vec{S}_i, \tag{3}$$

where S_c is the spin operator for the Cr^{3+} ion and S_i is the spin operator for the i^{th} Gd^{3+} ion, all in units of n.

The structure of $GdAlO_3$ is such that each Al^{3+} ion is surrounded by eight Gd^{3+} ions in an almost simple cubic arrangement. Since the distortion from cubic symmetry is small, we will assume that it is zero so that when a Cr^{3+} ion replaces an Al^{3+} ion, the interaction with all of the nearest neighbors Gd^{3+} ions is the same, i.e., $J_i = J$ for all i.

For the moment we will neglect the interactions between the Gd^{3+} ions. Our justification for this lies in the fact that the undoped $GdAlO_3$ is known to order antiferromagnetically at around 4°K whereas the principle features of the spectrum that we wish to describe are clearly evident at 77°K (Figure 5). We assume that the Cr^{3+} ion is exchange coupled to the eight nearest neighbors Gd^{3+} ions only.

The interaction defined in Equation 1 contains the spin operator for the Cr^{3+} ion and the spin operator for the eight Gd^{3+} ions. It is convenient to write it as

$$H' = - J \vec{S}_c \cdot S^+ \tag{4}$$

where

$$\vec{S} = \Sigma \vec{S}_i.$$

The matrix elements of an operator of the form $\vec{S}_c \cdot \vec{S}$ can be derived from the matrix elements of $|\vec{S}|^2$, $|\vec{S}_c|^2$, and $|\vec{S}_c + S|^2$ through the relation

$$2\vec{S}_c \cdot \vec{S} = |\vec{S}_c + \vec{S}|^2 - |\vec{S}_c|^2 - |\vec{S}|^2.$$

All eigenstates of the Hamiltonian H' are also eigenstates of $|\vec{S}_c + \vec{S}|^2$, $|S_c|^2$ and $|S|^2$, and the eigenvalues of H' are given by

$$- J \langle \mathcal{S}, S, S_c | \vec{S} \cdot \vec{S}_c | \mathcal{S}, S, S_c \rangle = - J \frac{\mathcal{S}(\mathcal{S}+1) - S(S+1) - S_c(S_c+1)}{2} \quad (5)$$

where $\mathcal{S}$ takes on all values $S + S_c$, $S + S_c - 1$, $\cdots\cdots$ $|S - S_c|$. When the Cr^{3+} ion is in its ground state, the spin is 3/2. The total spin values range, therefore, from $S + 3/2$ to $|S - 3/2|$. Substituting the possible values for $\mathcal{S}$ in Equation 5, we see that the energy levels of the four ground state bands are given by

$$\begin{aligned} E(S + 3/2) &= - 3/2\ JS, && S = 0 \text{ to } 28 \\ E(S + 1/2) &= 3/2\ J - J/2\ S, && S = 1 \text{ to } 28 \\ E(|S - 1/2|) &= 2J + J/2\ S, && S = 1 \text{ to } 28 \\ E(|S - 3/2|) &= 3/2\ J + 3/2\ JS, && S = 2 \text{ to } 28 \end{aligned} \quad (6a)$$

We will assume that the exchange coupling when the Cr^{3+} ion is in the ^2E state can be treated as if we had a simple non-degenerate spin 1/2 system.[25] The energy levels are then

$$\begin{aligned} E'(S + 1/2) &= E_o - J'/2\ S, && S = 0 \text{ to } 28 \\ E'(S - 1/2) &= E_o + J'/2 + J'/2\ S, && S = 1 \text{ to } 28 \end{aligned} \quad (6b)$$

egeneracy of the Eigenvalues

In a system of N ions each of which has an angular momentum of S_i, the number of angular momentum states that one can form is $(2S_i + 1)^N$ which in our case is 8^8 or 2^{24} since S = 7/2 for Gd^{3+} in the ground state and therefore each Gd ion may be in any of eight spin states. Each state of total angular momentum S will have the usual 2S + 1 degeneracy. Let us call the number of sets of these (2S + 1) states N(S). The numbers N(S) must satisfy the relation

$$\sum_{S=0}^{28} (2S + 1)N(S) = 8^8 \tag{7}$$

The sum over S runs from 0 to 28 since the maximum S corresponds to having all eight of the Gd^{3+} ions aligned, so that if we specify one component of S (say S_Z), then $S_{Zmax} = 8 \times 7/2 = 28$, and the minimum S is zero, corresponding to having four Gd ions anti-aligned with the remaining four.

In Appendix I, we show a procedure for calculating the number of ways (N(S)) of forming a state of total spin each with $S = S_o$. The results are contained in the following equations.

$$N(S) = N(S-1) + \sum_{I=o}^{4S_o-S} (2-\delta_{so})n(I+S)\, n(I) - \sum_{I=o}^{S-1} n(S-1-I)n(I), \quad 0 \leq S \leq 4S_o \tag{8a}$$

$$N(S) = N(S-1) - \sum_{I=o}^{8S_o-S+1} n(4S_0-I)n(S-1-4S_o+I), \qquad 4S_o \leq S \leq 8S_o \tag{8b}$$

where N(-1) = 0, δ is the Kronecker delta and

$$n(I) = (2S_o+1)(2I+1) - 3/2\ I(I+1), \quad 0 \leq I \leq 2S_o \tag{8c}$$

$$n(I) = \frac{(4S_o-I+1)(4S_o-I+2)}{2}, \qquad 2S_o \leq I \leq 4S \tag{8d}$$

The numbers N(S) for $S_o = 7/2$ are listed in Table I.IIIb of Appendix I. Each state of the eight Gd^{3+} ions with total spin S couples to the Cr^{3+} ion through the interaction H' (Equation 4) to form a final state of total spin δ. Each of these states has $(2\delta+1)$ components. Now since there are N(S) Gd^{3+} spin states of spin S, the total number of functions with total spin δ is

$$N(\ ) = (2\delta+1)N(S) \qquad (9)$$

and in our simple model these states are all degenerate. We therefore call this number the degeneracy. Using the N(S) values from Table I. IIIb, Equations (6a), (6b), and (9), we arive at a distribution of states of the Cr^{3+} - Gd^{3+} system shown in Figure 8.

Blazey and Burns[12] have calculated the $^4A_2$ density of states and used the expression (2S+1)N(S) rather than our Equation 9. Consequently they derived a distribution which is symmetric. On the basis of this they concluded that they were unable to determine the sign of the exchange parameters. We see in Figure 8 that the correct distribution is asymmetric.

It is evident from Figure 8 that the $S \pm 3/2$ bands are three times as wide as the $S \pm 1/2$ bands in the ground state bands. By averaging over a narrow band of levels we obtain a density of states that is shown in Figure 9 compared with the fluorescence spectrum at 4.2°K. A comparison suggests that the Cr^{3+} - Gd^{3+} coupling is ferromagnetic and a value of $J = 2.1\ cm^{-1}$ is obtained by matching the peak positions of the theoretical curve with the flourescence spectrum.

In matching the theoretical curve to the data, the effect of averaging the various S states over as wide a band as is indicated in Figure 9 resulted in raising the minimum between the two strongest bands as well as broadening the bands. This fitting procedure has obviously sacrificed the fit in the wings for a better fit in the center.

A similar comparison of the upper bands with the absorption spectrum again implies ferromagnetic coupling but here the exchange

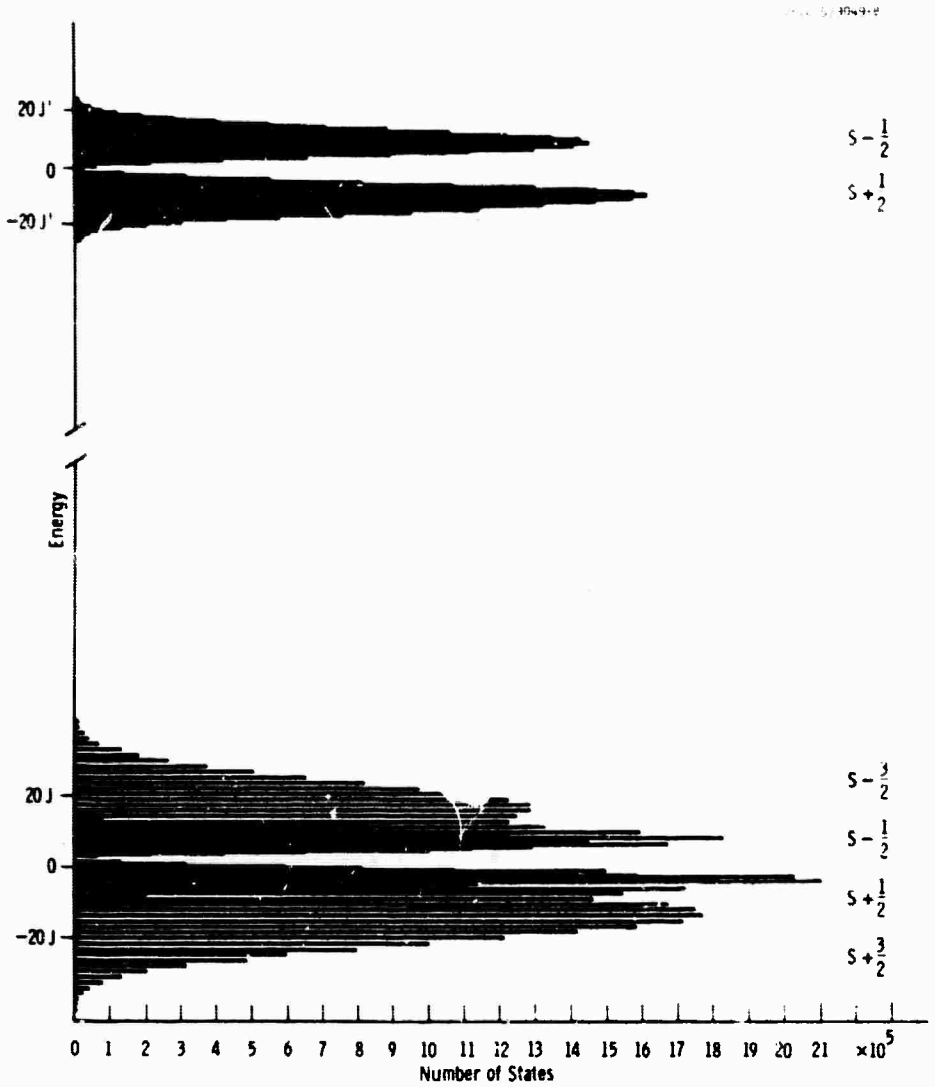

Figure 8

The Degeneracy of the Perturbation Hamiltonian $H' = -J\, S_c \cdot \sum_{i=1}^{\infty} S_i$ with $S_i = \frac{7}{2}$. In the Lower Manifold $S_c = 3/2$; in the Upper, $S_c = 1/2$.

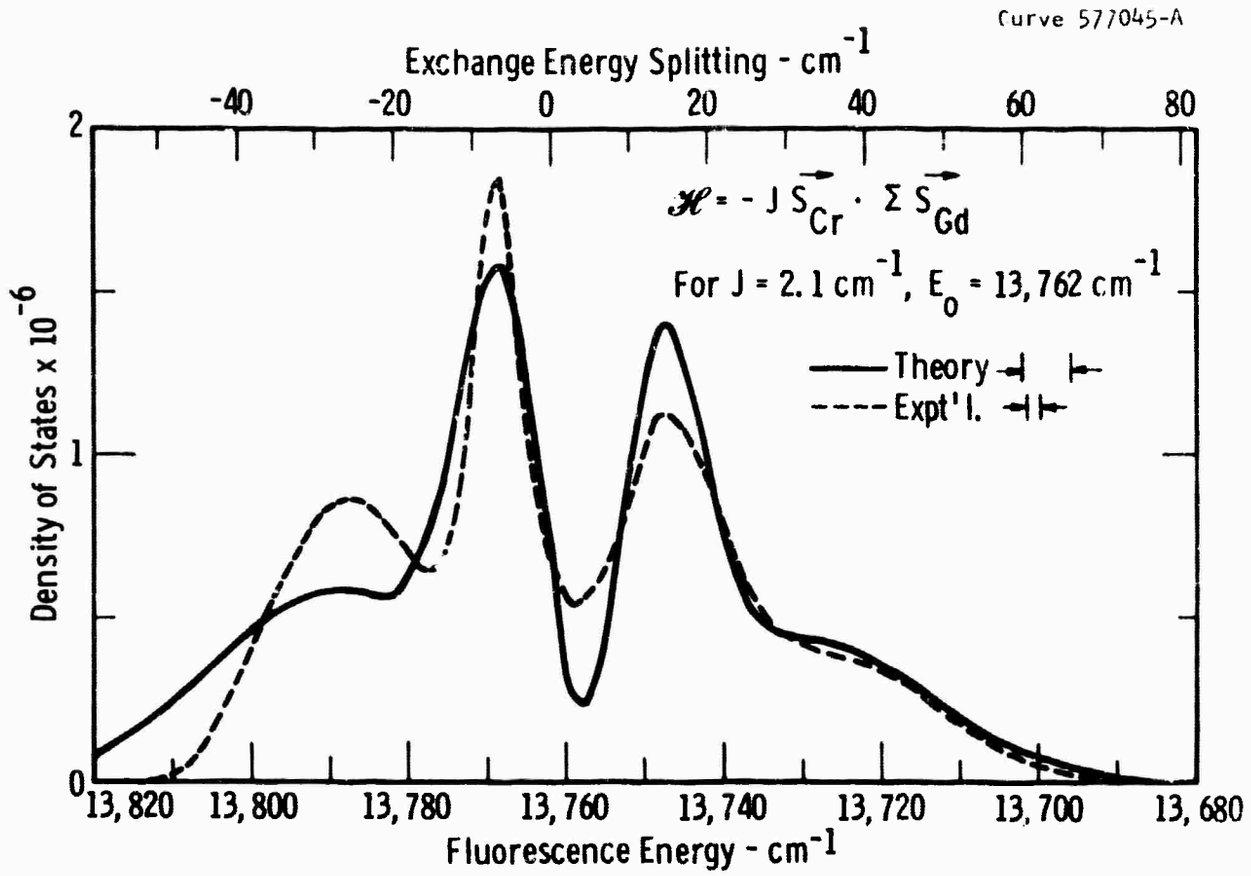

Figure 9

A Comparison of the Curve Obtained by Averaging the Lower Manifold in Figure 8 and Adjusting the Value of J to Match with the Observed Emission Spectrum.

coupling in the excited state must be $J' = 3.2\ cm^{-1}$. These numbers differ from those reported by Blazey and Burns[12] because as we have pointed out they have used the wrong density of states so that the peak to peak separations of their theoretical curve in units of the exchange parameters are incorrect.

It is evident that the simple model has features that relate to both the absorption and emission spectra. Notice in Figure 5 that as the temperature is raised to 77°K an additional band appears on the short wavelength side. The separation of the peak of this band from the peak of the nearest band to it is roughly equal to the separation between the peaks in the absorption spectrum. It seems reasonable to assume that this extra band arises from transitions between the S - 1/2 excited band to the S + 3/2 ground state band. The other transitions from the S - 1/2 excited band are superimposed on the transitions from the S + 1/2 band and presumably contribute to the excess width of the main peak at 77°K. There is an indication of a bump on the short wavelength side of the highest peak which is just where the S - 1/2 to S - 1/2 transitions would peak.

Selection Rules

The following considerations determine the selection rules for our simple model. Because the transitions involve the coupling of a Cr^{3+} moment to the electromagnetic field, the total spin, S, of the gadolinium ions is conserved. In the limit of low temperatures, we should then see four sharp lines in fluorescence, the long wavelength line noticeably weaker than the other three because of the selection rules on the chromium transitions. For example, it is known that for Cr^{3+} in Al_2O_3,[26] there is a selection rule on the chromium transitions, namely

$$\begin{aligned} |^2E, +1/2> &\leftrightarrow |^4A_2, -3/2> = 0 \\ |^2E, -1/2> &\leftrightarrow |^4A_2, +3/2> = 0 \end{aligned} \qquad (10)$$

VI. DISCUSSION

The fluorescence spectrum clearly does not consist of four sharp lines, nor the absorption spectrum, of two. A possibility (which we will shortly discard) is that the fluorescence and absorption spectra are inhomogeneously broadened i.e. each S state of the gadolinium is equally likely but a Cr^{3+} ion sees only one gadolinium configuration always i.e. the gadolinium system does not relax internally. The Cr^{3+}-Gd^{3+} system can relax by interacting with phonons in such a way that at T = 0°K only the S + 3/2 states are occupied when the Cr^{3+} is in the $^4A_2$ level and only the S + 1/2 states are occupied when the Cr^{3+} is the ^2E level. We can see from Equations (6a) and (6b) that the state separations between the components of the excited and the ground state bands are functions of the parameter S and therefore the fluorescence and absorption would consist of bands rather than sharp lines. In fluorescence, the restrictions given by Equation (10) lead to the condition that the S + 1/2 → S - 3/2 transitions are weak as are the S + 3/2 → S - 1/2 transitions in absorption.

The absorption corresponding to the $|S + 3/2| \rightarrow |S + 1/2|$ transitions should be identical with the $|S + 1/2| \rightarrow |S + 3/2|$ fluorescence spectra. We have measured (Figure 7) an incomplete overlap of the absorption and emission spectra. This suggests that the Gd environment does not preserve its total spin quantum number but that it relaxes towards the lowest energy levels before the fluorescence occurs. It is entirely reasonable that this relaxation should occur in the time scale of the fluorescence (∿ 9 ms at 2.2°K) since the Gd^{3+} ions are coupled together by exchange and magnetic interactions that do not conserve the total spin quantum numbers of the eight neighbors to Cr^{3+} ion. If the relaxation took place in an infinitessimally short time, every Cr^{3+} - Gd^{3+} system would find itself in the minimum energy level of the excited manifold just prior to fluorescence. To account for the fluorescence spectrum we would then have to allow that the spin selection rule on S^2 of the Gd environment is completely abolished and transitions are allowed from the bottom of the upper band to every level of the ground

manifold. This severe breakdown is not unacceptable in view of the S mixing nature of the Gd-Gd interactions. The limit of rapid relaxation would lead to the conclusion that the overlap between the absorption and emission spectrum should not be much greater than kT. The data shows an overlap of roughly 15 kT. Although this might indicate a condition intermediate between the "rapidly relaxing, S-mixing model" and the "non-relaxing, S conserving model", the overlap may be due to variations of $\pm$ 15% in the value of the exchange coupling parameters at different Cr^{3+} sites due to imhomogeneous strains. To determine whether such a variation in the J's can occur would require knowledge of the Cr^{3+}, O^{2-}, and Gd^{3+} wave functions in the crystal. This information is not available at present.

If it were the case that the Gd^{3+} system could relax only partially before the Cr^{3+} ion fluoresced, a change in the temperature should alter the Gd relaxation rate thereby altering the amount of overlap. Unfortunately, sufficiently detailed experiments have not been done to investigate this change; however, it would seem from a comparison of Figures 4 and 6 that there is not much difference between the extend of the overlap at 4.4° and at 2.15°K. Both the short wavelength emission and the long wavelength absorption shift to shorter wavelengths at the higher temperature.

We have so far found it necessary to deviate from our simple model to allow non-S conserving transitions. A spread in the J values can account for the overlap between the emission and absorption spectra. Let us now consider deviations of the Cr^{3+} environment from cubic symmetry. It has been mentioned that the space group of $GdAlO_3$ is D_{2h}^{16} - Pbnm. The pseudo cell that we have is generated by compressing a cube along the (110) direction and dilating it along the (1T0) direction. If the length of the unit cell in the (001) direction is left unchanged, we have, in distorting the cube in the manner prescribed, produced a T_{2g} distortion. The effect of such a distortion on the states of Cr^{3+} would be to mix the ^2E state with the $^4T_2$ and the $^4T_1$ states when taken in second order with the spin-orbit coupling. We are tempted to

attribute the decrease in lifetime and the increase in intensity of the fluorescence and the absorption spectrum to the increase in the distortion of the lattice from cubic symmetry as the system becomes magnetically order. However, further experiments are necessary to investigate this interpretation.

A further point to be made is that the larger admixture of ^4T states with the ^2E state due to a greater exchange interaction, the more depressed will be the latter state so that the emission will occur at longer wavelengths. The greater exchange coupling will also result in a greater spread in the density of states (Equations 6a and 6b). The combination of these two effects leads to a non-uniform change in the widths of the observed bands relative to the calculated density of states for a given set of J parameters in the ground and excited manifolds. To be specific the two long wavelength bands in emission should be broader than the shorter wavelength bands. This effect is observed (see Figure 6). Notice that as the temperature is lowered to 2.15°K the two highest peaked bands seem to be coming more equal in width. It is conceivable that the change in particle positions due to magnetic ordering might be appreciably greater than the variations from site to site due to inhomogeneous strains. If this is so, we can understand that the inhomogeneous strain effects would become less important as the crystal orders.

Magnetic Ordering of the Gd Lattice

It is known that[9,10,12] that $GdAlO_3$ orders antiferromagnetically at around 4°K. There is evidence in the fluorescence spectrum that the effects of this ordering affect the Cr^{3+} transitions by modifying the energies and eigenfunctions of the Gd^{3+} spins around the Cr^{3+}. The marked change in shape of both the absorption and emission spectra from 2° to 4°K is presumably due to this ordering. Notice in Figure 6 that the separations between the peaks decreases and the bands get narrower with decreasing temperature.

Blazey and Burns[12] have suggested that the decrease in peak separation implies a reduction of the Cr-Gd exchange coupling parameters.

Although this is a possibility, an alternate explanation might be that the Gd-Gd interactions, since they are antiferromagnetic, would tend to make the maximum Gd spin states higher in energy than the minimum spin states, thus narrowing each of the bands and reducing the separation between the peaks, as is observed. The fact that the radiative lifetime and the integrated absorption in the ^2E levels increase with decreasing temperature may be due to an increase in the Cr-Gd exchange interaction which, due to deviations from cubic symmetry at the Cr^{3+} lead to increased mixing of the ^2E levels with the higher more allowed bands. The effect of increasing the Cr-Gd exchange parameters on the distribution of energy levels could be compensation by the narrowing effects of the Gd-Gd interaction as discussed above.

VII. SUMMARY

The fluorescence and absorption spectra of $GdAlO_3:Cr^{3+}$ in the region of the $^2E \leftrightarrow {}^4A_2$ transitions consist of broad bands whereas in materials having nonmagnetic host metal ions, these transitions are sharp. The difference is attributed to an exchange interaction between the Cr^{3+} ion with its eight nearest neighbor Gd^{3+} ions. A simple model based upon an isotropic interaction of the form $-J\vec{S}_c \cdot \vec{S}$ where S_c denotes the spin of the chromium and S denotes the combined spin of the eight neighboring gadolimium ions, gives qualitative agreement between the density of states in the ground ($^4A_2$) manifold and the observed fluorescence spectrum as well as the density of states in the excited (^2E) and the absorption spectrum.

Deviations from the predictions of the simple model manifest themselves in the following ways:

1. If we assume that the Cr^{3+} environment can relax rapidly so that thermal equilibrium is established before the Cr^{3+} fluoresces, the selection rules predict at most four sharp lines. We observe four broad overlapping bands. In absorption we observe two broad bands whereas the model predicts two sharp lines.

2. If we assume that the environment of a Cr^{3+} ion is frozen in and cannot relax, the theory predicts a complete overlap between the shortest wavelength emission band and the longest wavelength absorption band. We observe only a partial overlap.

3. The rapidly relaxing model predicts overlap of only kT of the absorption and the emission at low temperatures. The observed overlap at 2.2°K is roughly 15 kT.

4. The lifetime of the emission decreases and the intensity of the absorption and the fluorescence increase as the temperature is lowered.

5. The width of the emission bands decrease with decreasing temperature.

We believe that the observations can be accommodated within an extend theory by introducing the following modifications:

1. The interaction between the gadolinium ions that results in the magnetic ordering of the lattice mixes all of the eigenstates of S^2 of the cube of gadolimiun ions surrounding the chromium. This interaction also allows the environment to relax so the fluorescence occurs from the bottom of ^2E manifold to all of the levels of the ^4A manifold of states.

2. The partial overlap between the emission and absorption spectrum is accounted for by allowing a distribution of strains about the Cr^{3+} ions resulting in a distribution in the values of the exchange parameters. The variations in the widths of the observed bands can also be attributed to these inhomogeneities.

3. The temperature dependence of the lifetime and intensities is thought to be due to the variation of the distortion of the crystal from cubic symmetry brought about by the magnetic ordering. The known crystal structure is of the right symmetry type to mix the ^2E states with the $^4T_1$ and $^4T_2$ states which are strongly coupled to the ground state by photons.

5. The variation of the width of the emission spectrum with temperature is thought to be caused by the competition between the Cr-Gd interactions and the Gd-Gd interactions. The former interactions tend to make the S = 28 state highest in energy. Above the Néel temperature, the Cr-Gd complex interactions with randomly oriented next nearest neighbors to the Cr^{3+}. This interaction averages to zero. As soon as the lattice starts to order, the average interaction no longer vanishes and so the states of eight nearest neighbors to the Cr^{3+} increase in energy.

The best fit to the data is obtained with a ferromagnetic coupling of the chromium ion to the nearest neighbor gadolinium ions. The values of the exchange parameters in the $^4A_2$ and ^2E states are 2.1 cm^{-1} and 3.2 cm^{-1} respectively. These values disagree with those published by Blazey and Burns who used an incorrect formula for the total number of coupled chromium-gadolinium states.

ACKNOWLEDGMENTS

The authors would like to thank R. Perevuznik, R. Muth, R. D. Haun, Jr., E. P. Reidel, and F W. Warren for their various contributions to the measurements and stimulating discussions throughout this work.

BLANK PAGE

FOOTNOTES AND REFERENCES

*Research supported under Project DEFENDER by The Advanced Research Projects Agency and the Office of Naval Research.

†Present address: Lockheed Research Laboratories, Palo Alto, California,

1. K. A. Wickersheim, in Magnetism, Vol. I, ed. by G. T. Rado and H. Suhl (Academic Press, New York, 1963) p. 269.

2. K. A. Wickersheim and R. L. White, Phys. Rev. Letters 4, 123 (1960); ibid 8, 483 (1962).

3. K. A. Wickersheim, Phys. Rev. 122, 1376 (1961); K. A. Wickersheim and R. A. Buchanan, J. Appl. Phys. 38, 1048 (1967).

4. A. J. Sievers, III and M. Tinkham, Phys. Rev. 124, 321 (1961); ibid 129, 1995 (1963).

5. P. L. Richards, J. Appl. Phys. Suppl. 34, 1237 (1963).

6. M. Tinkham, Phys. Rev. 124, 311 (1961).

7. J. J. Pearson and G. F. Herrmann, J. Appl. Phys. 38, 1067 (1967).

8. J. Mareschal, J. Sivardiere, and G. F. De Vries, presented at the International Conference on Magnetism, 1967 L. Holms, R. Sherwood and L. G. Van Uitert, ibid.

9. M. J. M. Leask, paper presented at the International Conference on Magnetism, 1967; S. Hufner, L. Holmes, [illegible]yi, and L. G. Van Uitert, Phys. Letters 25A, 301 (1967).

10. J. D. Cashion, A. H. Cooke, J. F. B. Hawkes, M. J. M. Leask, T. L. Thorp, and M. R. Wells, paper presented at the International Conference on Magnetism, 1967.

11. J. Murphy and R. C. Ohlmann, Optical Properties of Ions in Solids, (Wiley and Sons, N. Y. 1967) p. 60.

12. K. W. Blazey and G. Burns, Proc. Phys. Soc. (London), 91, 640 (1967).

13. S. Geller and V. B. Bala, Acta Cryst. 9, 1019 (1956).

14. W. Bagdade, private communication.

15. C. K. Jorgensen, Absorption Spectra and Chemical Bonding in Complexes, (Pergamon Press, New York, 1962); D. S. McClure, in Solid State Physics, Vol. 9, ed. by F. Seitz and D. Turnbull (Academic Press, New York, 1959) p. 399.

16. F. Forrat, R. Jansen, and P. Trevoux, Compt. Rend. 256, 1271 (1963); F. Forrat, G. Dauge P. Trevoux, G. Danner, and M. Christen, Compt. Rend. 259, 2813 (1964).

17. Corrections have been made for the shift of the peaks of the broad bands due to the slope of the background absorption. The values of the peak are those obtained at low temperatures--they are a few hundred cm^{-1} smaller at $300^{o}K$.

18. W. B. Fowler and D. L. Dexter, Phys. Rev. 128, 2154 (1962).

19. D. S. McClure, J. Chem. Phys.36, 2757 (1962).

20. Y. Tanabe and S. Sugano, J. Phys. Soc. (Japan) 9, 753,766 (1954).

21. In view of the uncertainty of these parameters it was not worthwhile to include the spin-orbit coupling interaction since it only shifts calculated energies by less than 100 cm^{-1}, whereas the uncertainty in the calculated energies are greater or equal to 100 cm^{-1}.

22. D. L. Wood, J. Ferguson, K. Knox, and J. F. Dillon, Jr. J. Chem. Phys. 39, 890 (1963).

23. H. Watanabe: Operator Methods in Ligand Field Theory (Prentice-Hall Int. Series in Chemistry) 1966; L. E. Orgel: An Introduction To Transition Metal Chemistry Ligand Field Theory (Wiley, N. Y., 1960).

24. L. Couture, F. Brunetiere, F. Forrat, and P. Trevoux, Compt. Rend. 256, 3046 (1963); R. C. Ohlmann, Bull. Am. Phys. Soc. 9, 281 (1964).

25. Despite the fact that the ^{2}E level is orbitally doubly degenerate we are correct to first order in treating each of the degenerate states as being independent of the other since the spin-orbit interaction within the ^{2}E states vanishes to first order in a cubic field. To this order the exchange coupling of the Cr^{3+} in the ^{2}E state to the Gd^{3+} can be treated as if all states were orbitally nondegenerate except that the density of states of the excited exchange coupled Cr^{3+} ion must be multiplied by a factor of 2.

26. G. F. Imbusch and S. Geshwind, Phys. Rev. Lett. 17 238 (1966).

TABLE I. Absorption Characteristics of Cr^{3+} in $GdAlO_3$

Final[a] State	λ Å	$\bar{\nu}$ cm^{-1}	σ(peak)[b] 10^{-20} cm^2 (2.2°K)	$\langle\bar{\nu}\rangle_{obs}$ cm^{-1}	$\langle\nu\rangle_{calc}$[c] cm^{-1}	$\int\sigma d\bar{\nu}$[b,d] 10^{-19} cm	f x 10^7[b,d]
$^2E(t_2^3)$	7241	13806	1.0	13820	13820	2.4(2°K)	1.4
	7235	18837	0.4		±300	1.4(4°K)	0.8
$^2T_1(t_2^3)$	6960	14364	1.1			10(2°K)	5.6
	6910	14468	0.45	14470	14320		
	6860	14577	0.1		±300	6(4°K)	3.4
$^4T_2(et_2^2)$	5500	18200 (±100)	4.0	18200 ±100	18200 ±100	900	510
$^2T_2(t_2^3)$	5006	19970	0.15	20000	21000	0.3(2°K)	0.2
	4990	20034	0.05		±300		
$^4T_1(et_2^2)$	4080	24500 ±100	8.3	24500 ±100	24500 ±100	2200	12400
$^4T_1(e^2t_2)$	2600	38000 ±1000	---	38000 ±1000	39200 ±500	---	---

[a] The lines attributed to $^2T_2(t_2^3)$ are too weak for positive identification; the $^4T_1(e^2t_2)$ position is only observed in excitation spectra.

[b] The chromium concentration was uncertain to ±30%; relative values are uncertain to ±10%.

[c] Calculated using Δ = 18200±100, B = 605±30, C = 3100±100 cm^{-1} from fit to $^4T_2(et_2^2)$, $^4T_1(et_2^2)$, and $^2E(t_2^3)$. C/B = 5.1±0.3.

[d] The integration is taken over all absorption lines for the doublet states.

TABLE II

The lifetime of the Cr^{3+} emission at various temperatures. The calculated values are obtained from the integrated absorption using Equation 2.

Temp °K	Lifetime Calc	Obs
2.2	7.3±2	9.0±.2
4.2	12.5±4	15.4±.3
77	-	18.0±.5
300	-	13.2±.5

TABLE III

A comparison of the Slater integrals F_2 and F_4 for Cr^{3+} in several hosts. All entries but the last two are derived from B anc C data reported by Wood et. al. (Ref. 22) using the defining equations $B = F_2 - 5F_4$ anc $C = 35\ F_4$.

Host	F_2 cm^{-1}	F_4 cm^{-1}
Free ion	1446	105
YAG	1111	94
YGaG	1056	97
Beryl	1203	85
K_2NaCrF_6	1191	86
$CrCl_3$	1036	97
$CrBr_3$	899	106
$LaAlO_3$	1041	86
$GdAlO_3$	1046	88

APPENDIX I

Van Vleck has described a method of determining the number of ways that N ions of spins S_o can be coupled together to form a state of total spin S. It consists of first finding the number of ways of forming a state of S_z by finding the coefficient of x^{S_z} in the expansion of

$$(x^{S_o} + x^{S_o-1} + x^{S_o-2} + \text{--------} x^{-S_o})^N \qquad \text{I-1}$$

Calling this number $\Omega(S)$ we find that the number of states with total spin S satisfies the relation

$$N(S) = [\Omega(S) - \Omega(S + 1)]\ (2S + 1) \qquad \text{I-2}$$

This procedure is awkward to use when dealing with as many as eight spin 7/2 ions. We have therefore derived a set of formulae that enable one to calculate these quantities simply for arbitrary S_o.

We begin by considering two ions of spin S_o coupled to form states varying in angular momentum from 0 to $2S_o$. For the moment we needn't consider the $2S_2 + 1$ possible projections of each total spin vector on any direction. The subscript 2 refers to a two-spin state. We say that out of two vectors there is only one resultant vector for each total spin from 0 to $2S_o$. The next step is to couple each pair state to a state from another pair to form a four-spin state of total spin S_4. In Table I-Ia we have listed across the top the minimum value of S_4 that the pairs of spins (S_2^i, S_2^j) in the corresponding column can form while at the left is shown the maximum S_4 that the pairs (S_2^i, S_2^j) in the corresponding row can form. The entries in Table I-Ib are the total numbers of pairs of the corresponding entries in Table I-Ia. Each entry in Table I-Ia where $S_2^i \neq S_2^j$ has the number 2 in the corresponding position in Table I-Ib. This number derives from the fact that for each pair (S_2^i, S_2^j) there is another pair (S_2^j, S_2^i). For those entries where $S_2^i = S_2^j$ there is only one pair for each i, hence the 1 entries in the (S_2^i, S_2^i) positions.

Now consider the total number of four-spin states of spin $S_4 = 0$. The only way to form a four-spin $S_4 = 0$ state is to use two equal S_2 vectors. The sum of the entries in the S = 0 column is the required number of $S_4 = 0$ states. The number of ways of forming a state of $S_4 = 1$ is found by adding the $S_4 = 1$ column of Table I-Ib to the $S_4 = 0$ and subtracting the $S_4 = 0$ row. This is so because each entry of Table I-Ia in columns $S_4 = 0$ and $S_4 = 1$ can form an $S_4 = 1$ state except the entry in the $S_4 = 0$ row. To find the number of $S_4 = 2$ states we add the $S_4 = 2$ column to the previous result and subtract the sum of the entries in the $S_4 = 1$ row. We continue this way until there are no more columns to add. When we arrive at this point we just continue to subtract rows until we exhaust the Table. By this time we will have calculated the number of ways of forming the state of maximum S_4. Since the state of maximum S_4 has all four spins aligned, it is obvious that there is only one way of doing it. The fact that the last quantity calculated must have the value 1 is a useful check on the results.

Tables I-Ia and I-Ib are applicable to the coupling of 4 spins of $s = 7/2$; however, from it we can deduce a formula appropriate to the coupling of four equal spins of arbitrary S value. As we have already pointed out, the sum of the entries in the $S_4 = 0$ column is the number of ways, n(0), of forming a state of spin $S_4 = 0$. In our present case this number is 3. For a general value of the S, this number would be $(2S_o + 1)$ as can be seen by examining the structure of Table I-Ia. According to our prescription, we find n(1) by adding the $S_4 = 1$ column and subtracting the $S_4 = 0$ row. In general we find n(I + 1) for I in the range $0 \leq I \leq 2S_o$

$$n(I + 1) = n(I) + 2(2S_o + 1) - 3I \qquad \text{I-3}$$

with $N(0) = 2S_o + 1$. When I is in the range $2S_o < I \leq 4S_o$, the recursion relation is

$$n(I + 1) = n(I) - (4S_o - I + 1) \qquad \text{I-4}$$

It is a simple matter to perform the sums indicated by these formula and when this is done we find

$$n(I) = (2S_o + 1)\,(2I + 1) - \frac{3}{2} I\,(I + 1) \qquad 0 \le I \le 2S_o \qquad \text{I-5a}$$

$$n(I) = \frac{(4S_o - I + 1)\,(4S_o - I + 2)}{2} \qquad 2S_o \le I \le 4S_o \qquad \text{I-5b}$$

The quantity $n(2S_o)$ is given correctly by either formula.

We have thus far coupled four spins S_o together to form all the states from $S_4 = 0$ to $S_4 = 4S$. Now we must couple two sets of S_4's together to form the state of S_8. The procedure is similar to that used for S_4. A table is composed with rows labeled by all the values of S_8 from 0 to $8S_o$ and with the columns with all the values from $S_8 = 4S_o$ to 0 starting from right to left as in Tables I-Ia and I-Ib. The entries in each column will be made up of all the pairs of vectors of S_4 that have in common that their minimum resultant spin that can be formed by combining the elements of the pair is given by the number labeling the column. Each pair of a row has in common with members of the same row the property that the maximum resultant spin is given by the number labeling the row. The resulting table is shown in Table I-IIa. Table I-IIb is derived as follows. As before, the entries of Table I-IIb are in a one-to-one correspondence with the entries of Table I-IIa. Consider any pair (S_4^i, S_4^j) in Table I-IIa. We have already found that there are $n(S_4^i)$ ways of forming the vector S_4^i and $n(S_4^j)$ ways of forming the vector S_4^j. There are, therefore, $n(S_4^i)\, n(S_4^j)$ pairs (S_4^i, S_4^j). If $i = j$ the entry in Table I-IIb is $[n(S_4^i)]^2$, however if $i \neq j$ we must multiply the $n(S_4^i)\, n(S_4^j)$ by 2 since the pair (S_4^i, S_4^j) is equivalent to the set (S_4^j, S_4^i). Each entry in Table I-IIa is therefore given by

$$\text{I-IIb } [i, j] = (2 - \delta_{ij})\, n(S_4^i)\, n(S_4^j) \qquad \text{I-6}$$

where δ_{ij} is the Kronecker δ. To find the number of ways of forming a state of $S_8 = S$ we add elements in a column subtract the sum of elements of a row as before. The results are given by

$$N(S) = N(S-1) + \sum_{I=0}^{4S_o - S} (2 - \delta_{S,o})\, n(I+S)\, n(I) - \sum_{I=0}^{S-1} n(S-I-1)\, n(I),$$

$$0 \leq S \leq 4S_o \qquad \text{I-7a}$$

$$N(S) = N(S-1) - \sum_{I=0}^{8S_o - S + 1} n(4S_o - I)\, n(I + S - 4S_o - 1),$$

$$4s \leq S \leq 8S_o \qquad \text{I-7b}$$

The value of $N(4S_o)$ is given by either formula. In these formulae $n(-1) = 0$ and the $n(I)$ are given by Equations I-5a and I-5b. The $n(S_4)$ and $N(S_8)$ value for eight $S_o = 7/2$ spins are listed in Tables I-IIIa and I-IIIb, respectively.

BLANK PAGE

S_{max} \ S_{min}	7	6	5	4	3	2	1	0
0								0,0
1							1,0	
2						2,0		1,1
3					3,0		2,1	
4				4,0		3,1		2,2
5			5,0		4,1		3,2	
6		6,0		5,1		4,2		3,3
7	7,0		6,1		5,2		4,3	
8		7,1		6,2		5,3		4,4
9			7,2		6,3		5,4	
10				7,3		6,4		5,5
11					7,4		6,5	
12						7,5		6,6
13							7,6	
14								7,7

Table I-Ia

The pairs (S_2^i, S_2^j) that form minimum values of S_4 given by the number labeling the column and maximum values of S_4 given by the number labeling the row.

7	6	5	4	3	2	1	0
							1
						2	
					2		1
				2		2	
			2		2		1
		2		2		2	
	2		2		2		1
2		2		2		2	
	2		2		2		1
		2		2		2	
			2		2		1
				2		2	
					2		1
						2	
							1

Table I-Ib

The number of pairs of vectors (S_2^i, S_2^j) for the corresponding entries in Table I-Ia.

S_{max} \ S_{min}	14	13	12	11	10	9	8	7	6	5	4	3	2	1	0
0															0,0
1														1,0	
2													2,0		1,1
3												3,0		2,1	
4											4,0		3,1		2,2
5										5,0		4,1		3,2	
6									6,0		5,1		4,2		3,3
7								7,0		6,1		5,2		4,3	
8							8,0		7,1		6,2		5,3		4,4
9						9,0		8,1		7,2		6,3		5,4	
10					10,0		9,1		8,2		7,3		6,4		5,5
11				11,0		10,1		9,2		8,3		7,4		6,5	
12			12,0		11,1		10,2		9,3		8,4		7,5		6,6
13		13,0		12,1		11,2		10,3		9,4		8,5		7,6	
14	14,0		13,1		12,2		11,3		10,4		9,5		8,6		7,7
15		14,1		13,2		12,3		11,4		10,5		9,6		8,7	
16			14,2		13,3		12,4		11,5		10,6		9,7		8,8
17				14,3		13,4		12,5		11,6		10,7		9,8	
18					14,4		13,5		13,6		11,7		10,8		9,9
19						14,5		13,6		12,7		11,8		10,9	
20							14,6		13,7		12,8		11,9		10,10
21								14,7		13,8		12,9		11,10	
22									14,8		13,9		12,10		11,11
23										14,9		13,10		12,11	
24											14,10		13,11		12,12
25												14,11		13,12	
26													14,12		13,13
27														14,13	
28															14,14

Table I-IIa

The pairs (S_4^i, S_4^j) that form minimum values of S_8 given by the number labeling the column and maximum values of S_8 given by the number labeling the row.

14	13	12	11	10	9	8	7	6	5	4	3	2	1	0
														64
													336	
												496		441
											608		1302	
										672		1596		961
									688		1764		2356	
								656		1806		2604		1444
							576		1722		2666		3192	
						448		1512		2542		3268		1764
					336		1176		2232		3116		3612	
				240		882		1736		2736		3444		1849
			160		630		1302		2128		3024		3526	
		96		420		930		1596		2352		3096		1681
	48		252		620		1140		1764		2408		2952	
16		126		372		760		1260		1806		2296		1296
	42		186		456		840		1290		1722		2016	
		62		228		504		860		1230		1512		784
			76		252		516		820		1080		1176	
				84		258		492		720		840		441
					86		246		432		560		630	
						82		216		336		420		225
							72		168		252		300	
								56		126		180		100
									42		90		120	
										30		60		36
											20		36	
												12		9
													6	
														1

Table I-IIb

The number of pairs of vectors (S_4^i, S_4^j) for the corresponding entries in Table I-IIa.

Table I-IIIa

The Number of Ways of Forming Vectors of Length S_4 Using Four Vectors $S_o = 7/2$

S_4	$n(S_4)$	S_4	$n(S_4)$
0	8	8	28
1	21	9	21
2	31	10	15
3	38	11	10
4	42	12	6
5	43	13	3
6	41	14	1
7	36		

Table I-IIIb

The Number of Ways of Forming Vectors of Length S_8 Using Eight Vectors $S_o = 7/2$

S_8	$N(S_8)$	S_8	$N(S_8)$	S_8	$N(S_8)$	S_8	$N(S_8)$
0	11,096	8	87,598	16	16,884	24	210
1	32,592	9	80,444	17	11,704	25	84
2	52,080	10	71,316	18	7,784	26	28
3	68,453	11	61,103	19	4,949	27	7
4	80,899	12	50,617	20	2,995	28	1
5	88,956	13	40,536	21	1,716		
6	92,532	14	31,368	22	924		
7	91,890	15	23,436	23	462		

APPENDIX B

CRYSTAL GROWTH OF $GdAlO_3$

R. Mazelsky and W. E. Kramer

I. INTRODUCTION

The compounds having perovskite type structures have long been of scientific interest. These compounds have found applications as ferroelectric and magnetic materials and, recently, have been thought to be possible laser host materials. For the latter use, the rare earth aluminum oxide perovskites were thought to be particularly promising as host for chromium.[1] Most of the rare earth-aluminum oxide perovskites were grown by solution techniques using molten salts as a solvent until recently Forrat et al[2] and Fay and Brandle[3] were successful in growing $LaAlO_3$ crystals from the melt by the Czochralski and Verneuill methods respectively. These crystals grew as twins due to a phase transition from rhombohedral to cubic occurring at approximately 400°C. A series of definitive papers on the structure of several families of perovskites including the rare earth aluminum oxides were written by Geller and co-workers.[4,5,6] In these papers the structure of the various perovskite type compounds were clarified and a relation was tentatively established between ionic sizes and the occurrence of the rhombohedral and cubic structure. A less clear relationship was observed between the orthohombic, rhombohedral, and cubic forms of the perovskite although it was proposed that an orthorhombic structure would first go through a transformation to the rhombohedral form before a cubic perovskite would be obtained.

II. PREPARATION

Gadolinium oxide and aluminum oxide advertised 99.999% purity were mixed together and melted in an iridium crucible. An approximate melting point was obtained by means of a series of pyrometer readings

uncorrected for emissivity and was found to be approximately 2050°C. The melt on freezing could not readily be removed from the crucible. Since there was no visible attack on the crucible nor any significant loss in weight of the crucible on removal of the charge even after eight hours, the iridium was thought to be a suitable crucible container. A sample of the boule resulting from the melt was ground into powder and an x-ray powder photograph was taken. Within the limits of the method the photograph was that of $GdAlO_3$ only with no other phases observed. The lines were indexed ' 'attice parameters were calculated. The results were in good agreem th Geller's data on an orthorhombic cell having the dimensions a = 5.247, b = 5.304 and c = 2.447. Successive meltings and x-ray data showed only $GdAlO_3$. This was taken to indicate that $GdAlO_3$ is a congruently melting compound which lends itself to growth from the melt.

III. CRYSTAL GROWTH

The apparatus for the growth of refractory oxide crystals has been described elsewhere.[7] The power source was a Westinghouse 10 kHz, 30 kw motor generator set. This low frequency was found to be quite beneficial for high temperature growth due to the large penetration depth of the field with the result that small crucible irregularities did not result in hot spots. As a result crucible life was extended for several runs even at crucible temperature estimated at 2200°C.

For all pulling runs the crucible was 1/2 to 2/3 full. By proper positioning of the crucible in the coil a thermal gradient of approximately 50°C was maintained on the crucible. The temperature of the crucible wall as measured with a pyrometer was approximately 50° cooler at the top of the crucible than at the liquid level. When the charge was completely molten, a distinct grapefruit pattern was observed on the surface of the melt which has been related to convective instability by Bardsley and Cockayne.[8] This pattern was partially disrupted on dipping of the seed.

Preliminary growth runs were made using a polycrystalline seed of $GdAlO_3$ cut from an ingot of previously melted material. The seed was necked in and then broadened into approximately 1/4" diameter. Pulling and rotation rates were 1 cm/hr and 40 rpm respectively. On cooling the crystal remained clear until approximately red heat after which point cracks were observed in the boule. On cooling to room temperature the crystal became opaque due to the large number of cracks. A small transparent area remained and this was used as a seeding for succeeding runs. Several crystals were grown of approximately 1/4" diameter and 1/2" to 1-1/2" long. In all cases in standing at room temperature for times varying from 1 to 48 hours, cracks developed and optical quality pieces larger than a centimeter could not be retained. Cooling rates of the pulled crystal were varied from 2 to 6 hours with no effect on the tendency of the boule to crack. Crystals were also grown off-stoichiometry on both the gadolinium and aluminum excess side of $GdAlO_3$ without any apparent effect.

Chromium was added to the melt in concentrations of 0.001, 0.01, and 0.1 atom % as a substitute for aluminum. The crystals obtained also showed a marked tendency to crack. Spectroscopic data on chromium doped $GdAlO_3$ is described in the preceding appendix to this report.

IV. DISCUSSION

It is not clear whether the crystal's propensity for cracking is due to strains in the crystal or a high temperature phase transition. A small hole was bored in an ingot of $GdAlO_3$ and a thermocouple was inserted. A second thermocouple was used to monitor temperature of the furnace. A multipoint recorder was used to monitor temperature in this furnace and simultaneously in the $GdAlO_3$ while the furnace was cycled between 500°C and 1500°C at about 100°C per hour. No anomaly was observed in temperature indicating there is no rapid phase transformation at these temperatures.

Geller[4,5,6] has described the phase relationships among compounds of the perovskite structure, ABO_3, where A is a rare earth trivalent ion and B is a trivalent transition metal ion. None of these are cubic at room temperature, the structures being rhombohedral or orthorhombic. The three symmetries are closely related to one another and it is a relatively simple matter to work with nearly cubic pseudocells of all the compounds. Geller has looked at the rare earth aluminum oxide series and has approximated a critical volume for the "aluminates" at which they become cubic. This volume for the simple pseudocubic cell is approximately 56 Å^3 this value being derived from the compounds $LaAlO_3$, $SmAlO_3$, and $PrAlO_3$. The volume expansion as a function of temperature has been determined for these compounds and they are the same within 10%. If one assumes that the same relations given above hold in the $GdAlO_3$ system, one can estimate the temperature at which $GdAlO_3$ will become cubic. This temperature is above the melting point and is estimated at between 2200°C and 2600°C.

Empirically, it is therefore unlikely that a cubic transformation occurs in the solid range. However, there is some evidence that the orthorhombic structure will undergo a phase transition to rhombohedral before the cubic phase appears. Geller does not make any estimates of volume relations between the orthorhombic and rhombohedral phases. However, it is possible that there is such a transition below the melting point. It is, therefore, difficult to determine if the phase transition is responsible for the cracking of the crystals or if the cracking is due to simple mechanical strain. The thermal analysis did not show an energy anomaly to 1500°C. However, the transformation, if it exists, may be sluggish or at temperatures above this point.

A slice of one of the crystals is shown in Fig. 10. Twin boundaries are visible in the photograph and they show a triangular shape. Back reflection Laue photographs indicate that this phase is the 111 of the orthorhombic cell. This slice was cut perpendicular to the pull

Figure 10

Photograph of a Slice of a $GdAlO_3$ Crystal
Showing Twin Boundaries

direction of a crystal nucleated in a polycrystalline seed. An examination of the orthorhombic and rhombohedral structures does not show any obvious relationship as to why the twin boundaries should form in this way if a phase transition took place. Therefore, it is not possible to distinguish between a mechanical twin or one due to a phase transition.

V. CONCLUSION

The results on the growth of $GdAlO_3$ are not clear although it is possible to grow large transparent crystals, the strains due to growth, impurities, or a phase transition cause severe cracking. Sufficient information has not been acquired to determine the source of the strain.

REFERENCES

1. Ohlmann and Murphy, Appendix A this report.

2. Forrat, Jansen and Trevoux, Compte Rendu, 1271, Feb. 4 (1963).
3. Fay and Brandle, Proc. ICCG, 51, H. S. Perser, Pergamon Press (1967).
4. S. Geller and V. B. Bala, Acta Cryst. 9, 1019 (1956).
5. S. Geller and V. B. Bala, Acta Cryst. 10, 243 (1951).
6. S. Geller and V. B. Bala, Acta Cryst. 13, 248 (1957).
7. Mazelsky, Ohlmann and Steinbruegge, accepted for publication in J. Electrochem. Soc.
8. Bardsley and Cockayne, Proc. ICCG, 109, H. S. Peeser, Pergamon Press (1967).

BLANK PAGE

Unclassified
Security Classification

DOCUMENT CONTROL DATA - R&D

(Security classification of title, body of abstract and indexing annotation must be entered when the overall report is classified)

1. ORIGINATING ACTIVITY (Corporate author)	2a. REPORT SECURITY CLASSIFICATION
Westinghouse Research Labs Pittsburgh, Pa. 15235	Unclassified
	2b. GROUP

3. REPORT TITLE

High Energy Crystalline Laser Materials

4. DESCRIPTIVE NOTES *(Type of report and inclusive dates)*

Final Technical Summary Report 10/16/65 - 3/3/67

5. AUTHOR(S) *(Last name, first name, initial)*

Ohlmann, R.C.; Mazelsky, R.; Murphy, J.

6. REPORT DATE	7a. TOTAL NO. OF PAGES	7b. NO. OF REFS
12/1/67	51	34

8a. CONTRACT OR GRANT NO.	9a. ORIGINATOR'S REPORT NUMBER(S)
Nonr-4658(00)	67-9C1-LXTLS-R1
b. PROJECT NO. ARPA Order 306	
c. Code 4730	9b. OTHER REPORT NO(S) *(Any other numbers that may be assigned this report)*
d. Req. No. NR-017-721/ 11-21-65	--------

10. AVAILABILITY/LIMITATION NOTICES

Qualified requesters may obtain copies of this report from DDC

11. SUPPLEMENTARY NOTES	12. SPONSORING MILITARY ACTIVITY
	Advanced Research Projects Agency and Office of Naval Research, Washington, D.C.

13. ABSTRACT

A potential high energy laser material, $GdAlO_3$ doped with chromium, is discussed in terms of its growth problems and spectroscopic characteristics. Crystals have been pulled from the melt, but difficulties in maintaining stochiometry during growth have not been completely solved. The fluorescence of Cr^{3+} has an 18 msec decay time and a broad R-line. The width and structure of the R-lines are theoretically described as due to the ferromagnetic exchange interactions with neighboring Gd^{3+} ions.

DD FORM 1 JAN 64 1473

Unclassified
Security Classification

RM 35054

14 KEY WORDS	LINK A		LINK B		LINK C	
	ROLE	WT	ROLE	WT	ROLE	WT
Lasers						
Fluorescence						
Spectroscopy						
Chromium						
Crystals						
Exchange Interaction						
Gadolinium Aluminum Oxide						

INSTRUCTIONS

1. ORIGINATING ACTIVITY: Enter the name and address of the contractor, subcontractor, grantee, Department of Defense activity or other organization *(corporate author)* issuing the report.

2a. REPORT SECURITY CLASSIFICATION: Enter the overall security classification of the report. Indicate whether "Restricted Data" is included. Marking is to be in accordance with appropriate security regulations.

2b. GROUP: Automatic downgrading is specified in DoD Directive 5200.10 and Armed Forces Industrial Manual. Enter the group number. Also, when applicable, show that optional markings have been used for Group 3 and Group 4 as authorized.

3. REPORT TITLE: Enter the complete report title in all capital letters. Titles in all cases should be unclassified. If a meaningful title cannot be selected without classification, show title classification in all capitals in parenthesis immediately following the title.

4. DESCRIPTIVE NOTES: If appropriate, enter the type of report, e.g., interim, progress, summary, annual, or final. Give the inclusive dates when a specific reporting period is covered.

5. AUTHOR(S): Enter the name(s) of author(s) as shown on or in the report. Enter last name, first name, middle initial. If military, show rank and branch of service. The name of the principal author is an absolute minimum requirement.

6. REPORT DATE: Enter the date of the report as day, month, year; or month, year. If more than one date appears on the report, use date of publication.

7a. TOTAL NUMBER OF PAGES: The total page count should follow normal pagination procedures, i.e., enter the number of pages containing information.

7b. NUMBER OF REFERENCES: Enter the total number of references cited in the report.

8a. CONTRACT OR GRANT NUMBER: If appropriate, enter the applicable number of the contract or grant under which the report was written.

8b, 8c, & 8d. PROJECT NUMBER: Enter the appropriate military department identification, such as project number, subproject number, system numbers, task number, etc.

9a. ORIGINATOR'S REPORT NUMBER(S): Enter the official report number by which the document will be identified and controlled by the originating activity. This number must be unique to this report.

9b. OTHER REPORT NUMBER(S): If the report has been assigned any other report numbers *(either by the originator or by the sponsor)*, also enter this number(s).

10. AVAILABILITY/LIMITATION NOTICES: Enter any limitations on further dissemination of the report, other than those imposed by security classification, using standard statements such as:

(1) "Qualified requesters may obtain copies of this report from DDC."

(2) "Foreign announcement and dissemination of this report by DDC is not authorized."

(3) "U. S. Government agencies may obtain copies of this report directly from DDC. Other qualified DDC users shall request through _____."

(4) "U. S. military agencies may obtain copies of this report directly from DDC. Other qualified users shall request through _____."

(5) "All distribution of this report is controlled. Qualified DDC users shall request through _____."

If the report has been furnished to the Office of Technical Services, Department of Commerce, for sale to the public, indicate this fact and enter the price, if known.

11. SUPPLEMENTARY NOTES: Use for additional explanatory notes.

12. SPONSORING MILITARY ACTIVITY: Enter the name of the departmental project office or laboratory sponsoring *(paying for)* the research and development. Include address.

13. ABSTRACT: Enter an abstract giving a brief and factual summary of the document indicative of the report, even though it may also appear elsewhere in the body of the technical report. If additional space is required, a continuation sheet shall be attached.

It is highly desirable that the abstract of classified reports be unclassified. Each paragraph of the abstract shall end with an indication of the military security classification of the information in the paragraph, represented as *(TS), (S), (C), or (U)*.

There is no limitation on the length of the abstract. However, the suggested length is from 150 to 225 words.

14. KEY WORDS: Key words are technically meaningful terms or short phrases that characterize a report and may be used as index entries for cataloging the report. Key words must be selected so that no security classification is required. Identifiers, such as equipment model designation, trade name, military project code name, geographic location, may be used as key words but will be followed by an indication of technical context. The assignment of links, rules, and weights is optional.